



Influence of Process Parameters on Compression Properties of 3D Printed Polyether-Ether-Ketone by Fused Filament Fabrication

Erika Lannunziata^(✉) , Alberto Giubilini , Abdollah Saboori ,
and Paolo Minetola 

Integrated Additive Manufacturing Centre (IAM@PoliTO), Department of Management and Production Engineering (DIGEP), Politecnico di Torino, Corso Duca degli Abruzzi 24, 10129 Torino, Italy

Erika.lannunziata@polito.it

Abstract. Metal replacement is an effective approach for sustainable manufacturing of polymer products in various sectors with the key advantage of reducing the component weight. Technopolymers are a class of materials with increased properties, i.e., thermal and chemical stability as well as mechanical resistance, compared to traditional plastics, thus resulting in a more efficient alternative for metal parts. Nowadays, Additive Manufacturing is a game-changer production technology due to its high flexibility, geometrical accuracy, reduced time and costs, and minimal waste. Therefore, an attractive research topic for technopolymers is their application in Additive Manufacturing. Polyether-ether-ketone (PEEK) is a semi-crystalline technopolymer, its thermal susceptibility during the cooling step of the process remains the dominant cause of dimensional warping and job failure. The nozzle and bed/chamber temperature difference should be optimised to reduce the thermal gradient. Previous researchers investigated the nozzle and bed temperature effects deeply. However, the chamber temperature influence on the dimensional accuracy and compression properties is still missing in the literature, particularly for samples printed with an infill lower than 100%. Therefore, this study aims to fill these gaps and deepen the knowledge about PEEK printing via Fused Filament Fabrication by evaluating the effects of chamber temperature and infill percentage over compression properties, printing accuracy and energy consumption. The specific compression properties highlighted that the highest values were reached for not fully dense samples. Furthermore, the heating chamber did not affect the dimensional accuracy and compressive properties as strongly to justify an energy consumption increment of 45%.

Keywords: Fused Filament Fabrication (FFF) · PEEK · Additive Manufacturing · Compression properties · X-ray Computed Tomography

1 Introduction

The metal-to-plastic conversion, or metal replacement, has recently attracted the interest of the industrial world from the automotive sector to the biomedical one for a more sustainable manufacturing transition [1]. Moreover, plastics have been considered an

interesting alternative to metals for purposes of saving weight, cost, and time processing. Since its introduction in the late 1980s, Poly-ether-ether-ketone (PEEK) has attracted lots of attention from industries [2]. PEEK is a high-performance thermoplastic polymer consisting of an aromatic backbone molecular chain, which imparts a special resistance to high temperatures and chemical attacks, interconnected by ketone and ether functional groups conferring flexibility and manufacturability [3]. Consequently, the physical and mechanical qualities of PEEK make it a potential option for substituting metal in a wide range of high-performance end-use applications [4]. With its high Young's modulus, tensile strength, and low specific gravity, PEEK can replace aluminium or steel in various applications, including aerospace and automotive [5].

Furthermore, PEEK is biocompatible, easily sterilisable, radio-transparent, and it possesses a Young modulus closer to that of bones compared to metals. For all these properties, it is a promising material for biomedical applications, particularly as an appropriate alternative to precious metal implants [6]. The fundamental drawback of conventional manufacturing processes is their lack of flexibility in producing components with elaborate designs. In this regard, the advancement of Additive Manufacturing (AM) techniques nowadays makes it possible to manufacture components in PEEK with design freedom in an affordable way. Among the AM technologies, Fused Filament Fabrication (FFF) is the most commonly used for fabricating thermoplastic parts based on CAD designs. In this process, a polymeric filament is continuously driven through a heated print head, where it is softened and extruded through a nozzle to build the part layerwise on a heated platform. This additive technique offers low manufacturing cost, freedom in design, and supervision-free operation. Recently, great effort has been put into PEEK production by FFF. Previous investigations on the 3D printing of PEEK showed promising outcomes [7], although its thermal susceptibility during manufacturing remains the most significant obstacle. PEEK's semicrystalline nature consists of well-ordered crystalline zones mixed with amorphous regions, which exhibit lower density, tensile strength, Young's modulus, and stress cracking resistance than the crystalline domains. The percentage of crystallinity strongly depends on the thermal gradient that occurs during the crystallisation phase in the process of cooling from the melt state [8]. Thus, the nozzle and bed/chamber temperature difference during 3D printing should be optimised to improve the mechanical properties and dimensional accuracy of PEEK. As reported in a previous study [7], the nozzle temperature is a crucial parameter for dimensional accuracy, the crystallisation process, and interfacial strength between layers. The optimum range for the nozzle temperature was identified between 420 and 440 °C. It is well documented that a further increment could result in PEEK thermal degradation [7, 8]. The melted polymer from the nozzle is deposited on the bed, whose temperature promotes diffusion bonding among adjacent filaments and affects the surface topography of PEEK parts [9]. In order to reduce the thermal gradient between the nozzle and the bed, the chamber temperature should be higher than the ambient temperature. Wang et al. [10] demonstrated how high chamber temperature positively affected PEEK crystallinity, resulting in better mechanical properties. These results were related to the tensile tests, and the compression properties reference is still missing in the literature. The temperature dependence of PEEK in 3D printing has been studied only for a part

infill of 100%, lower infill percentages were not included in the thermal investigation [11, 12].

Therefore, this work aims to fill these gaps and contribute to deepening the knowledge about PEEK printing via FFF by evaluating the effects of the chamber temperature and infill percentage. Furthermore, dimensional accuracy and time and energy consumption were considered to provide a comprehensive evaluation that can help broaden the diffusion of metal replacement with PEEK by taking advantage of innovative manufacturing technologies, such as Fused Filament Fabrication.

2 Materials and Method

The PEEK filament used in this study is the PEEK K10 produced by Kexcelled (North Bridge New Material Technology, Sozhou, China). According to the material manufacturer's data sheet, the filament had a diameter of 1.75 ± 0.02 mm and a density of 1.28 g/cm^3 . Before processing, the spool was oven dried at $80 \text{ }^\circ\text{C}$ overnight to remove environmental moisture. The 3D printer used for manufacturing all the samples was the CreatBot PEEK-300 (CreatBot, Zhengzhou, China), which has a building volume of $300 \times 300 \times 400 \text{ mm}^3$, heatable up to $150 \text{ }^\circ\text{C}$. Furthermore, this machine has a double nozzle that allows the processing of both traditional polymers as well as technopolymers, which require high processing temperatures up to $500 \text{ }^\circ\text{C}$. The 3D printed samples were cylinders with a diameter of 10 mm built from the platform plate (XY) and a height of 10 mm (Z-axis), with reference to Type B specimen of the ISO 604 guideline [13]. The cylinder samples were designed on Solidworks software and then imported into Simplify 3D software for the slicing procedure. Four different infill percentages were identified, respectively 30%, 50%, 70% and 100%, and for each value, six samples were produced with the printing parameters summarised in Table 1.

Table 1. Process parameters used for the fabrication of all specimens.

Parameter	Value
Nozzle temperature [$^\circ\text{C}$]	420
Bed temperature [$^\circ\text{C}$]	140
Printing speed [mm/s]	25
Layer height [mm]	0.2
Infill pattern	Rectilinear
Infill angle [$^\circ$]	± 45

Under the same printing conditions, two different sets of samples were produced with the chamber heated to $140 \text{ }^\circ\text{C}$ and without heating. Henceforth, the first set of samples will be referred to as "HC" and the second set as "CC" with reference to the hot chamber or cold chamber, respectively. The dimensional accuracy was analysed by comparing the nominal CAD geometry with the tomography scans acquired with a

micro-CT scan model Phoenix vltomelx S240 (GE Baker Hughes-Waygate Technologies, Wunstorf, Germany). The compression tests were carried out using an AURA 5T machine (Easydur, Arcisate, Italy) performed according to the ISO 604 standard [13] at a test speed of 5 mm/min to evaluate the compressive strength and establish up to 70% strain deformation of the specimen. Five samples were 3D printed and tested for each infill percentage and chamber temperature condition. MATLAB software was used to calculate the compression modulus for each sample by evaluating the initial slope of the compressive curves in the elastic region.

3 Results

Dimensional Accuracy. Dimensional characterisation of all 3D printed specimens was preliminary conducted with a micrometre, as well as the weight measurement, through a Gibertini 1000HR-CM balance. The results are listed in Table 2, along with the printing time and the energy consumption (EC) of specimen production, which was measured using a Meterk M34EU power meter plug for each infill percentage and thermal condition (TC) of the printing chamber.

The analysis of these results verified the evident increasing influence of weight, printing time, energy consumption, and infill percentage. There is no significant effect of chamber temperature on printing time, whereas its influence on the energy consumption required to print each sample is evident. In fact, consumption increases up to 63% for the samples with 30% infill. Dimensional accuracy was confirmed by tomography analysis, whose scans are illustrated and compared to the nominal CAD model in Fig. 1. The results showed that extra material extrusion occurred by increasing the infill percentage, even up to reaching an over-extrusion in the case of 100% infill percentage. This phenomenon can be related to an unsuitable extrusion speed, which causes the spreading of extra material from the nozzle resulting in oversized printed samples [3]. From the tomography results,

Table 2. Dimensional evaluation, weight, printing time, and energy consumption (EC) of all 3D printed samples in different thermal conditions (TC).

TC	Infill [%]	Diameter [mm]	Height [mm]	Weight [g]	Printing time [min per sample]	EC [kWh per sample]
CC	30	9.70 ± 0.08	9.90 ± 0.04	0.58	7	0.16
	50	9.84 ± 0.08	9.86 ± 0.07	0.72	8	0.17
	70	9.76 ± 0.07	9.82 ± 0.04	0.85	9	0.2
	100	10.16 ± 0.03	10.13 ± 0.03	1.01	11	0.22
HC	30	9.72 ± 0.07	9.81 ± 0.00	0.58	7	0.26
	50	9.77 ± 0.01	9.64 ± 0.01	0.72	8	0.27
	70	9.71 ± 0.07	9.61 ± 0.01	0.85	9	0.29
	100	10.17 ± 0.05	10.02 ± 0.01	1.02	11	0.31

and specifically evaluating the cumulative distribution at 90 % of the deviation between the nominal surface and the actual one (Table 3), it is possible to observe that the chamber heating (HC) increased the deviation. This effect could be explained by an increment of crystallinity due to slower cooling because of the hot chamber, thus suggesting a suitable scaling during the definition of the part design. Therefore, 50% and 70% infill percentage samples, with no heated chamber (CC), produced more accurate samples by saving time and energy at the same speed.

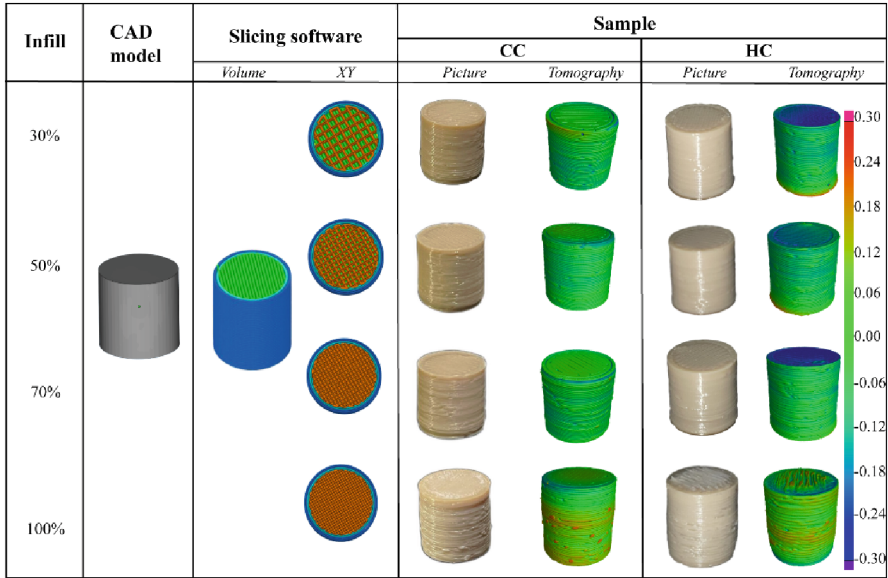


Fig. 1. Comparison of CAD model, printing paths in the slicing software, and tomographic scans with the chromatic representation of deviation between actual and nominal dimensions of the different samples.

Table 3. 90% of the cumulative deviation distribution between the nominal surface and the actual one of the samples at varying infill percentage and chamber condition (TC).

90% of the cumulative distribution of deviation		
Infill [%]	CC	HC
30	0.16 mm	0.15 mm
50	0.12 mm	0.16 mm
70	0.13 mm	0.19 mm
100	0.17 mm	0.18 mm

Compressive Properties. The compressive performance of 3D printed samples was characterised by compression tests, and the main findings are shown in Fig. 2 for the lowest and highest infill percentages and both chamber conditions (TC). Table 4 summarises the compressive strengths and modulus, as well as their values normalised according to sample mass and considered as specific values. All the compressive stress and strain curves (Fig. 2) displayed three defined regions: (I) a linear elasticity zone, (II) a plateau region, and (III) a densification region. After the first elastic deformation (I), during the second phase (II), the internal structure of the samples deformed with almost no increase in density. It can be observed from Fig. 2 that the length of the plateau decreases proportionally with the increase of the infill percentage due to a higher amount of extruded material and, thus, a greater possibility of internal rearrangement of the structure. In the third stage (III), stress increased rapidly without a significant increase in deformation since the samples began to compress as bulk material, resulting in a rapid increase in the sample response. These results of the experimental tests are consistent with previous research in the literature [14], and, as expected, the compressive performance increased for increasing infill percentages. The compressive strength evaluated at a 70% strain increased from 91.3 ± 10.1 for 30% infill to 306.1 ± 17.4 MPa for 100% infill. A similar trend was also observed for the compressive modulus, ranging from 651.5 ± 16.1 to 1197.3 ± 49.9 MPa.

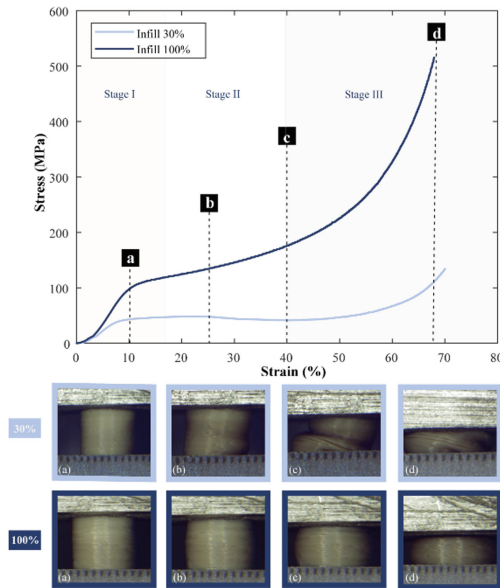


Fig. 2. Compressive behaviour of the lowest infill percentage (30%) and the highest one (100%).

For a thorough and significant interpretation of these results, it is better to correlate them with their specific values, normalised according to the sample mass. Figure 3 highlights the differences between the values of compressive properties and the specific

ones for different infill percentages. The 30% infill corresponded to the lowest amount of material subjected to deformation, leading to the weakest response under load, as Fig. 2c shows with the sample crush. Considering the specific compressive properties, it is worth noting that up to 70% infill, there is always an improvement in the compressive behaviour. Beyond this value, the deposited material seems to give a less significant contribution, and therefore the 100% infill samples display a lower specific compressive modulus than 70% infill ones. These results are consistent with previous findings [15]. The chamber temperature also slightly improved the compressive properties in the order of about 10% for each infill percentage. The effect of chamber temperature on mechanical properties appears to be in contrast to what has been previously reported in the literature [11, 12]. One possible explanation for this result could be related to the small dimensions of the 3D printed geometries, which are significantly affected by the temperature of the heated plate and the nozzle maintained at a temperature higher than 400 °C [16].

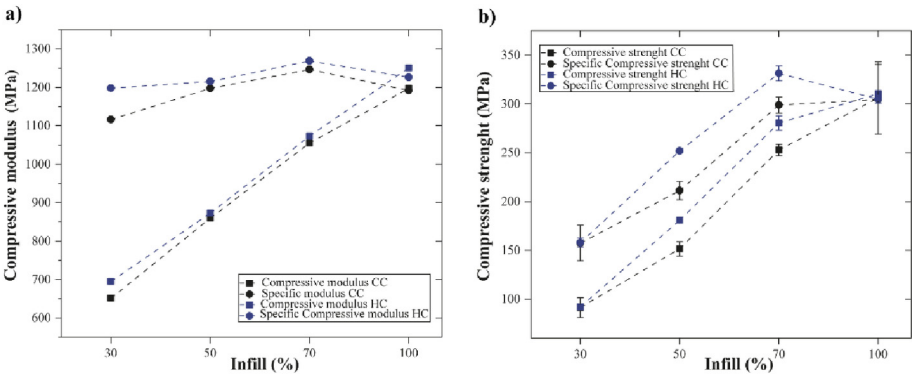


Fig. 3. (a) the compressive modulus and its specific values, (b) the compressive strength and its specific values for each infill and thermal conditions.

Table 4. Compressive performance of the specimens for four different infill percentages (30%, 50%, 70%, 100%) and two chamber conditions (TC).

TC	Infill [%]	Compressive strength [MPa]	Compressive modulus [MPa]	Specific compressive strength [MPa/g]	Specific compressive modulus [MPa/g]
CC	30	91.3 ± 10.1	651.5 ± 16.1	157.4 ± 18.3	1116.5 ± 26.6
	50	151.6 ± 7.2	859.6 ± 27.5	211.2 ± 9.3	1197.3 ± 33.5
	70	252.8 ± 6.0	1055.3 ± 31.9	298.8 ± 8.2	1246.8 ± 39.9
	100	306.1 ± 17.4	1197.3 ± 49.9	304.6 ± 35.9	1192.0 ± 55.9
HC	30	92.1 ± 2.8	695.0 ± 12.1	157.9 ± 4.6	1197.9 ± 27.2
	50	180.8 ± 1.5	872.7 ± 31.4	251.7 ± 1.8	1214.9 ± 47.7
	70	280.5 ± 7.4	1073.3 ± 18.0	331.3 ± 7.7	1269.0 ± 26.0
	100	310.2 ± 3.4	1250.7 ± 5.1	304.7 ± 4.1	1226.5 ± 3.8

4 Conclusions

This work examined the infill percentage and the chamber heating impact on the dimensional accuracy, printing time, and energy consumption required for 3D printing PEEK compressive sample by FFF. Additionally, the compressive properties were investigated for different infill percentages with and without a heated 3D printing chamber. Based on the outcomes, it can be concluded that the infill percentage affected the dimensional accuracy, reaching an over-extrusion for the 100% infill samples, probably due to an unsuitable extrusion speed. Therefore, the extrusion speed might be increased for a high infill percentage to reduce the dimensional deviations from the nominal CAD model. 50% and 70% infill percentages pointed out to have the lowest cumulative deviation of the specimen surface to the nominal dimensions at the printing speed used in this study. Even considering the compression performance, the highest specific properties were reached for the samples with 70% infill, achieving time and material savings compared to fully dense cylinders. Furthermore, the heating chamber slightly improved the compressive properties up to a maximum of 10% increase. However, considering an average increase in energy consumption of about 45% resulting from the heating chamber, we can conclude that the compressive strength improvement did not justify the consumption increment for the sample designed in this study. The findings of this preliminary study are promising results that pave the way for further research, which should investigate the effect of the heating chamber on different sample geometries, e.g., with larger specimen dimensions or at higher chamber temperatures.

References

1. Carvalho, M.: EU energy and climate change strategy. *Energy* **40**(1), 19–22 (2012)
2. Verma, S., Verma, S., Sharma, N., Kango, S., Sharma, S.: Developments of PEEK (polyetheretherketone) as a biomedical material: a focused review. *Eur. Polym. J.* **147**(15), 110295 (2021)
3. Wang, Y., Müller, W.D., Rumjahn, A., Schwitalla, A.: Parameters influencing the outcome of additive manufacturing of tiny medical devices based on PEEK. *Materials* **13**(2), 466 (2020)
4. Yang, C., Tian, X., Li, D., Cao, Y., Zhao, F., Shi, C.: Influence of thermal processing conditions in 3D printing on the crystallinity and mechanical properties of PEEK material. *J. Mater. Process. Technol.* **248**, 1–7 (2017)
5. Shekar, R.I., Kotresh, T.M., Rao, P.D., Kumar, K.: Properties of high modulus PEEK yarns for aerospace applications. *J. Appl. Polym. Sci.* **112**(4), 2497–2510 (2009)
6. Han, X., et al.: Carbon fibre reinforced PEEK composites based on 3D-printing technology for orthopaedic and dental applications. *J. Clin. Med.* **8**(2), 240 (2019)
7. Zanjanijam, A.R., Major, I., Lyons, J.G., Lafont, U., Devine, D.M.: Fused filament fabrication of peek: a review of process-structure-property relationships. *Polymers* **12**(8), 1665 (2020)
8. Jin, L., Ball, J., Bremner, T., Sue, H.J.: Crystallization behaviour and morphological characterisation of poly (ether ether ketone). *Polymer* **55**(20), 5255–5265 (2014)
9. Wang, P., Zou, B., Ding, S.: Modeling of surface roughness based on heat transfer considering diffusion among deposition filaments for FDM 3D printing heat-resistant resin. *Appl. Therm. Eng.* **161**, 114064 (2019)
10. Wang, R., Cheng, K.J., Advincula, R.C., Chen, Q.: On the thermal processing and mechanical properties of 3D-printed polyether ether ketone. *MRS Commun.* **9**, 1046–1052 (2019)

11. Wu, W.Z., Geng, P., Zhao, J., Zhang, Y., Rosen, D.W., Zhang, H.B.: Manufacture and thermal deformation analysis of semicrystalline polymer polyether ether ketone by 3D printing. *Mater. Res. Innov.* **18**, S5-12 (2014)
12. Hu, B., et al.: Improved design of fused deposition modelling equipment for 3D printing of high-performance PEEK parts. *Mech. Mater.* **137**, 103139 (2019)
13. EN ISO 604. Plastic Determination of Compressive Properties (2002)
14. Ait-Mansour, I., Kretschmar, N., Chekurov, S., Salmi, M., Rech, J.: Design-dependent shrinkage compensation modelling and mechanical property targeting of metal FFF. *Prog. Addit. Manuf.* **5**, 51–57 (2020)
15. Gao, R., Xie, J., Yang, J., Zhuo, C., Fu, J., Zhao, P.: Research on the fused deposition modelling of polyether ether ketone. *Polymers* **13**(14), 2344 (2021)
16. Basgul, C., Thieringer, F.M., Kurtz, S.M.: Heat transfer-based non-isothermal healing model for the interfacial bonding strength of fused filament fabricated polyetheretherketone. *Addit. Manuf.* **46**, 102097 (2021)